Research Paper | Open Access

An application of Auto-regressive (AR) model in predicting Aero-elastic Effectsof Lekki Cable Stayed Bridge

Hassan Abba Musa [1], Dr. A. Mohammed[2]

[1]*Civil Engineering Department, Sharda University, Knowledge Park III, Greater Noida, UP – Delhi, India.*
[2] *Department of Civil Engineering, Abubakar Tafawa Balewa University (ATBU) Bauchi, Bauchi, Nigeria.*

ABSTRACT: *In current practice, the predictive analysis of stochastic problems encompasses a variety of statistical techniques from modeling, machine, and data mining that analyse current and historical facts to make predictions about future. Therefore, this research uses an AR Model whose codes are incorporated in the MATLAB software to predict possible aero-elastic effects of Lekki Bridge based on its existing parametric data and the conditions around the bridge. It was seen that, the fluctuating components of the wind velocity as displayed by the fluctuant curve will result in the vibration of the structure, even strengthening the resonance effect of the structure. Therefore, it suggested that, the natural frequency of the bridge should be set aside far from system frequency considering direct parametric excitation of pedestrian or vehicular traffic speed.*

Key Words: Predictive Analytics,Stochastic, AR Model, MATLAB, Aero-elastic Effects, Lekki Bridge,Fluctuant curve.

I. INTRODUCTION

Cable structures are encountering a growing success in modern Engineering due to technical, economic and aesthetic reasons, which justify their actual competitiveness for covering free spans in an increasingly wide length range. The structural and architectural design of suspended and cable-stayed bridges, in particular, has been fine tuned over the last few decades to conjugate efficient geometric shapes, optimal material usage, and appreciable visual pleasantness. Focusing on the structural view points, the virtuous synergy among the load-bearing capacity of beams (or arches) and the force transferring ability of cables has been optimally exploited in a variety of collaboration schemes (Fig. 1.1a). Nonetheless, this optimization trend often ends up over-stressing the inherent properties of slenderness and flexibility of cable supported bridges and footbridges. Such structural features, combined with low damping capacities and associated with rising performance demands due – among other things – to the increase of live loads, thus make these structures particularly vulnerable to dangerous dynamic phenomena, including for instance the aero-elastic instabilities due to wind actions, or the dynamic bifurcations due to the direct or parametric excitation of pedestrian or vehicular traffic.

The non-negligible influence of the cable vibrations on the free and forced full-bridge dynamics is a key-issue, well recognized since the early nineties of the past century [1]. Consequently, a variety of continuous and discrete formulations have been proposed to overcome the inherent shortcomings of traditional models, coarsely describing the cables as tendon elements with Ernst equivalent elastic modulus [2, 3]. The matter tends to become determinant in the newest structural realizations, considering that the modern design trend is to prevent the risk of stress localization in the suspension system (main cables, arch, towers) by increasing the total number of suspending cables. In this respect, several numerical and experimental studies confirm that cable-supported bridges typically possess a dense spectrum of natural frequencies, in which internal resonant conditions among global modes, dominated by the flexural and or torsional dynamics of the deck (Fig. 1.1b), and local modes, dominated instead of the lateral dynamics of one or more cables (Fig. 1.1c), are practically unavoidable [4].

In this challenging scenario, it may be worth devoting some theoretical research efforts to develop structural models able to well balance the competing requirements of synthesis and representativeness, with expected positive spill overs in a variety of engineering applications, including vibration controls and health monitoring systems.
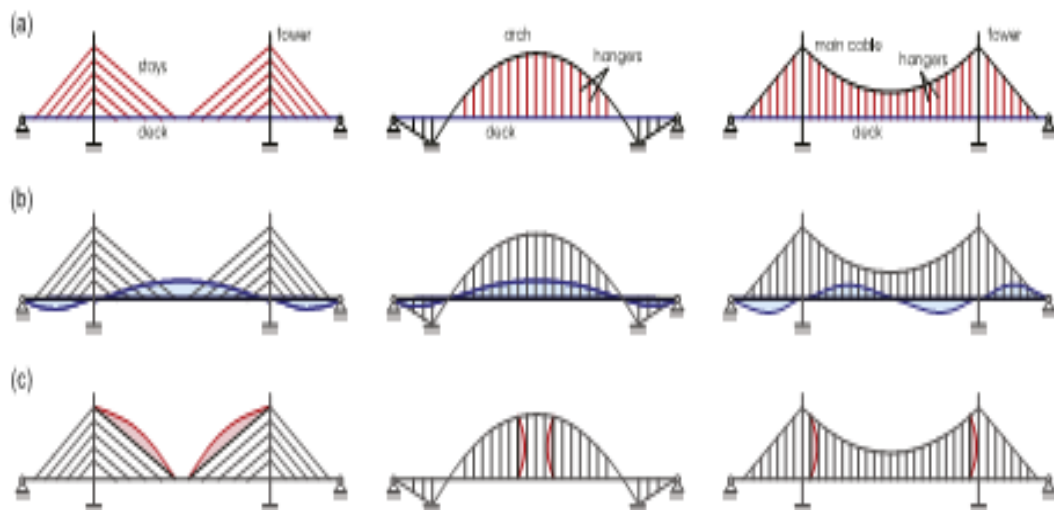
Figure 1.1: Cable-stayed bridge (left), Through-arch bridge (centre), suspended bridge (right); qualitative examples of (a) cable-beam collaboration schemes, (b) deck vibration shape in global modes, (c) cable vibration shapes in local modes (Marco et al, 2014).

In comparison with the current state-of-the-art, the present work will discuss the mostcommon phenomena related to wind effects bridge of Lekki cable-stayed bridges, Lagos; thereby underlining the prominent roles of the dynamics of the structures.

II.   0BACKGROUND OF THE RESEARCH

When designing flexible structures for wind, dynamic wind loads are of primary interest to structural Engineers. Wind loads are induced on a structure because of a complex interaction between wind and structure. The interaction of wind flow with structures can be classified under aerodynamic and aero-elastic effects (Scanlan 1981, Simiu and Scanlan 1996) [5]. The **Aerodynamic Effect** refers to the fluctuating nature of the wind and itsinteraction with the structure. The discipline of **Aero-elasticity** refers to the phenomenon wherein aerodynamic forces and structural motions interact significantly. Aero-elastic instability occurs if the body that is immersed in the fluid flow deflects under some force and the initial deflection causes succeeding deflections that are divergent in character. Aero-elastic instabilities also involve aerodynamic forces that are generated due to the motion of the structure. These forces that act upon a body as a consequence of itsmotion and cause aero-elastic instability are termed as self-**excited forces**. The self-excited wind loads will either transfer energy from wind to the structural motion or help in dissipating the kinetic energy of the structure.Above a certain wind speed, the energy increment exceeds the energy dissipation from wind such that the kinetic energy of the structure keeps increasing which makes the structure dynamically unstable. This critical wind speed at which the structure becomes unstable is called **Flutter Speed**.

2.1 FLUTTER INSTABILITY

Since the flutter induced failure of the Tacoma Narrows Bridge in 1940, understanding of the physical mechanisms at work in Civil Engineering structures has advanced tremendously. Flutter is an aero-elastic self-excited oscillation of a structural system. The structural system by means of its deflections and their time derivatives taps off energy from the wind flow across the body. If the system is given an initial deflection, its motion will either decay or diverge according to whether the energy of motion extracted from the wind is less than or exceeds the energy dissipated by the system through mechanical damping. The theoretical dividing line between the decaying and divergence (i.e. sustained sinusoidal oscillation) was identified as the **Critical Flutter Condition.**

Flutter phenomenon can be broadly classified into two categories, namely, single-degree-of-freedom flutter or damping driven flutter example like torsional flutter of bluff bodies(bluff-sectioned) bridges, and coupled-flutter or stiffness driven flutter example like multi-mode flutter of structures airplane (wings and streamlined) bridges. Flutter analysis of a structure can be performed either in frequency domain or in time domain.

2.1.1 FREQUENCY-DOMAIN FLUTTER ANALYSIS

The frequency-domain flutter analysis approach has been widely used for estimating flutter speed of structures. The frequency-domain analysis using flutter derivative formulation for the aero-elastic forces was researched extensively by Sarkar, Jones, and Scanlan (1994), Jones et al. (1995), Matsumoto et al. (1997), Scanlan (1997), Gu, Zhang, and Xiang (2000), Zhu et al. (2002) and numerous others. Mode-by-mode flutter analysis was done by Ge and Tanaka (2000), Jones and Scanlan (2001) [5]. The frequency domain

method uses flutter derivatives which are functions of reduced frequency. These aero-elastic parameters can be experimentally obtained from wind-tunnel testing of section models.

2.1.2 TIME-DOMAIN FLUTTER ANALYSIS

For frequency domain flutter analysis technique, the resulting equations of motion involve reduced frequency dependent coefficients. Thus, the analysis requires iterative search for the critical flutter wind speed. Moreover, material and geometric nonlinearities in the structural system cannot be incorporated into the frequency domain flutter analysis. Also, the design of vibration suppression systems is hindered due to the reduced frequency dependence.Time domain flutter analysis, that uses frequency independent state-space equations to represent the equations of motion, is gaining popularity in recent times because:

• Flutter analysis does not require iterative calculations while solving the complex eigenvalue problem to determine the frequencies, damping ratios, and mode shapes at different velocities,

• Structural and aerodynamic nonlinearities can be incorporated in the analysis.

•The time domain formulation can be used to design vibration control systems for suppressing flutter phenomenon that are more efficient.

III. METHODOLOGY

3.1 AUTO-REGRESSIVE (AR) MODEL

Fluctuating wind loads, which mostly relate to the shape and height of the structure, are (multi points) random loads and one of the main dominating excitations of large structures in civil engineering. In any study of buffeting and flutter analysis of structures, the wind velocity is indispensably considered, but an accurate wind velocity model usually requires expensive cost through a full ruler observation or a wind tunnel experiment. Therefore, it is significant to study the wind effects simulation by numerical simulation methods.

The AR model was applied mostly to forecast the time history series in wind engineering, because of its many benefits: simple algorithm and rapid calculation; besides, it can consider not only the space dependent characteristic, but also the time dependent characteristic of the **wind history**, and also those advantages can be simplistic to implement by **computer programming like Matlab**. Though the Autoregressive Moving Average (ARMA) is superior to the AR model, the parameter estimation for the ARMA model is much more difficult than the AR model. Hence, this work will concern with the issues of the AR model while using it to simulate the natural wind velocity processes.

Figure 3.1: Lekki cable stayed bridge (Julious Berger Plc, 2013)

Therefore, this paper attempts to present the corresponding solving methods whose computing programs are implemented in MATLAB Code based on the case study of Lekki link cable stayed bridge, and the method used in deducing AR model by matrix form in simulating the wind velocity of the spatial 3-D fields are all referred to the **Appendix A and Appendix B** respectively.

3.2 SIMULATION OF RANDOM WIND VELOCITY FIELD ON CABLE STAYED BRIDGES BASED ON AUTO-REGRESSIVE (AR) MODEL

The fluctuating wind velocity is a random time series in essence. The basic formula of the wind velocities $u(t)$ at M spatial points, idealized as stationary Gaussian multivariate stochastic processes, it can be expressed as [6, 7, and 8]:

$$[u(t)] = \sum_{k=1}^{p} [\psi_k][u(t - k\Delta t)] + [N(t)] \quad \dots \text{(3.1)}$$

Where $[N(t)] = [N^1(t), \dots, N^M(t)]^T$, $[N^i(t)]^T$ is the ith normally distributed stochastic process with zero mean and unit variance, $i = 1, \dots, p$ is the rank of AR model, and Δt is the time step of the series. The process of the simulation can be realized as follows.

3.2.1 CALCULATION OF COEFFICIENT MATRIX $[\psi_k]$

After multiplying the two sides of Eq. 3.1 by $[u(t - j\Delta t)]$ and calculating the expectation, we can get the following formula:

$$E\{[u(t)][u(t - j\Delta t)]\} = E\{\sum_{k=1}^{p}[\psi_k][u(t - k\Delta t)][u(t - j\Delta t)]\} + E[[N(t)][u(t - j\Delta t)]\} \quad \dots \text{(3.2)}$$

Since the covariance between stochastic process $u(t)$ and $u(t - j\Delta t)$ can be expressed as $R_u(j\Delta t) = E[\{u(t) - E[u(t)]\}\{u(t - j\Delta t) - E(u(t - j\Delta t))\}] = E[u(t)(u(t - j\Delta t)]$, and the stochastic process $N(t)$ is independent to stochastic wind velocity $u(t)$, then the relationship between the covariance $R_u(j\Delta t)$ and regressive coefficient $[\psi_k]$ can be written as:

$$R_u(j\Delta t) = \sum_{k=1}^{p}[\psi_k][R_u(j - k)\Delta t)] \quad \dots \text{(3.3)}$$

In which $j = 1, 2 \dots P$. after transpose, Eq. (3.3) can be rewritten in the matrix form:

$$[R] = [\overline{R}][\psi] \quad \dots \text{(3.4)}$$

Where

$$[R]_{pM\times M} = [R_u(j\Delta t), \dots, R_u(p\Delta t)]^T$$

$$[\psi]_{pM\times M} = [\psi_1^T, \dots, \psi_p^T]^T$$

$$[\overline{R}]_{pM\times pM} = \begin{bmatrix} R_u(0) & R_u(\Delta t) & \cdots & R_u[(P-2)\Delta t] & R_u[(P-1)\Delta t] \\ R_u(\Delta t) & R_u(\Delta t) & \cdots & R_u[(P-3)\Delta t] & R_u[(P-2)\Delta t] \\ \vdots & \vdots & \ddots & \vdots & \vdots \\ R_u[(P-2)\Delta t] & R_u[(P-3)\Delta t] & \cdots & R_u(0) & R_u(\Delta t) \\ R_u[(P-1)\Delta t] & R_u[(P-2)\Delta t] & \cdots & R_u(\Delta t) & R_u(0) \end{bmatrix} \quad \dots \text{(3.5)}$$

In which

$$[R_u(j\Delta t)] = \begin{bmatrix} R_u^{11}(j\Delta t) & \cdots & R_u^{1N}(j\Delta t) \\ \vdots & \ddots & \vdots \\ R_u^{M1}(j\Delta t) & \cdots & R_u^{MM}(j\Delta t) \end{bmatrix}, [\psi_j] = \begin{bmatrix} \psi_j^{11} & \cdots & \psi_j^{1M} \\ \vdots & \ddots & \vdots \\ \psi_j^{M1} & \cdots & \psi_j^{MM} \end{bmatrix} \quad \dots \text{(3.6)}$$

According to random vibration theory, the relationship between the **power spectral density** and the **correlation function** accords with the Wiener-Khinchin theorem [9]:

$$R_u^{ik}(j\Delta t) = \int_0^{\infty} S_u^{ik}(f) \cos(2\pi.f.j\Delta t) df \quad \dots \text{(3.7)}$$

Where f is the frequency, $S_u^{ik}(f)$ is the auto-power spectral density if $i = k$, the cross-power spectral density if $i \neq k$, $k = 1, 2, \dots, M, j = 1, \dots, p$. The study of this term may be simplified by assuming that the imaginary component of the cross-spectrum is negligible for the purposes of the study that is to be carried out:

$$S_{ij}(f) = \sqrt{S_{ii}(f).S_{jj}(f).coh_{ij}(f)} \quad \dots \text{(3.8)}$$

Where $coh_{ij}(f)$ represents the coherence function of longitudinal fluctuations at points i and j of the plane orthogonal to the mean wind direction. As described, the three-dimension expression of the coherence function is:

$$coh_{ij}(f) = \exp\left[\frac{-2f\sqrt{C_x^2(x_i-x_j)^2 + C_y^2(y_i-y_j)^2 + C_z^2(z_i-z_j)^2}}{\overline{U}(z_i) + \overline{U}(z_j)}\right] \quad \dots \text{(3.9)}$$

Where, C_x, C_y, and C_z, are the appropriate decay coefficients. For the purpose of this present study, the following values were adopted $C_x = 8$ (longitude direction), $C_y = 16$ (transverse direction), and $C_z = 10$ (vertical direction).

3.2.2 CALCULATION OF THE NORMALLY DISTRIBUTED RANDOM PROCESSES $N(t)$

The normally distributed random processes $N(t)$ can be obtained from:

$$[N(t)] = [L][n(t)] \quad \dots \text{(3.10)}$$

Where $[n(t)] = [n_1(t), n_2(t), \dots, n_m(t)]^T$, $n_i(t)$ is the ith independent normally distributed random process with zero mean and unit variance, in which $i = 1, 2, \dots, M$; $[L]$ is from the Cholesky decomposition of $[R_N] = [L][L]^T$, in which $[R_N]$ is calculated from the following equation obtained by multiplying two sides of Eq. (3.1) with $[u(t)] = [u^1(t), \dots, u^M(t)]^T$

$$[R_N] = [R_u(0)] - \sum_{k=1}^{p}[\psi_k][(R_u(k\Delta t)] \quad \ldots\ldots \ (3.11)$$

3.2.3 CALCULATION OF THE FLUCTUATING WIND VELOCITY

Using the results of Eq. 3.2 and Eq. 3.8, with the presumption of $u^i(t) = 0$, while $t < 0$, Eq. 3.1 can be dispersed and rewritten as:

$$\begin{bmatrix} u^1(h\Delta t) \\ \vdots \\ u^M(h\Delta t) \end{bmatrix} = \sum_{k=1}^{p}[\psi_k]\begin{bmatrix} u^1(h-k)\Delta t) \\ \vdots \\ u^M(h-k)\Delta t) \end{bmatrix} + \begin{bmatrix} N^1(h\Delta t) \\ \vdots \\ N^M(h\Delta t) \end{bmatrix} \quad \ldots\ldots \ (3.12)$$

$h = 0, 1, 2 \ldots$ and $k = 1, \ldots, p$ in which Δt is the time step.

3.2.4 CALCULATION OF THE FINAL WIND VELOCITY

The final wind velocity can be generated by:

$$U(t) = \overline{U} + u(t) \quad \ldots\ldots \ (3.13)$$

Where, $\overline{U}$ is the mean component of wind velocity.

3.5.5 SELECTION OF THE AR MODEL RANK

Iwatani point out that the low rank of the AR model can meet the requirement in general engineering with the permitted error [6]. But, for large and complex structures, it is not credible to solve the rank of AR model based on the empirical analysis only. However, much work has already been done and many experimental results have been given. Ref [10, 11, and 12] proposed a new method to select the AR model order by translating the n-variate AR model equations into **state-spaceform**. Different from those former works ref [15] developed a new method of resolving the rank of AR model based on the principle of the AIC (Akaike Information Criterion). The AIC can be expressed as:

$$AIC(p) = \ln \sigma_a^2 + 2p/N \ \ldots\ldots \ (3.14)$$

Where N is the sample time length, σ_a^2 is the variance.

With the increasing rank of the AR model initially, the value of the variance σ_a^2 and AIC(p) decrease. However, the value of AIC(p) will increase with the rising rank. Hence, P_0 is taken as the best rank of the AR model if it is determined by the formula for a special rank, m.

$$AIC(P_0) = \sum_{1 \le p \le m} \min AIC(p) \ldots\ldots \ (3.15)$$

It is a huge job to calculate the variance σ_a^2 for a multidimensional sequence. In this study, it is proposed that the variance σ_a^2 can be replaced by the absolute of the maximum eigenvalue of the matrix $[R_N]$.

3.2.6 IMPLEMENTATION OF THE AR MODEL

There are two important points in the implementations of the AR model based on the MATLAB programming: (Fig 3.2).

3.2.6.1 SOLVING THE ILL-POSED EQ. 3.4 RESULTING FROM THE INCREASING DEGREES OF FREEDOM OF THE STRUCTURE

Eq. 3.4 can be solved by a general iterative method for a structure with a few degree freedoms. However, the large dimension of the coefficient matrix [R], which results from a large number of degrees of freedom, will make the Eq. 3.4 an ill conditioned equation. Therefore the complicated method with better accuracy is needed for resolving the problem. Here, over relaxation iteration [13] is used to calculate the large sparse matrix equation. The iteration formula of the algorithm is:

$$\psi_{ij}^{k+1} = (1-\omega)\psi_{ij}^{k} + \frac{\omega}{r_{ij}}\left[\overline{r_{ij}} - \sum_{l=1}^{i=1} r_{ij}.\psi_{lj}^{k+1} - \sum_{l=i+1}^{pM} r_{il}\psi_{lj}^{k}\right] \quad \ldots\ldots \ (3.16)$$

Where ω is the relaxation factor which controls the convergent rate of the iteration algorithm, $i = 1, 2, \ldots, M$. With the condition of positive definite matrix [R], the formula would be convergent with $1 < \omega < 2$. It is suggested that the relaxation factor value should be within the range of $1.0 \sim 1.05$ in this study.
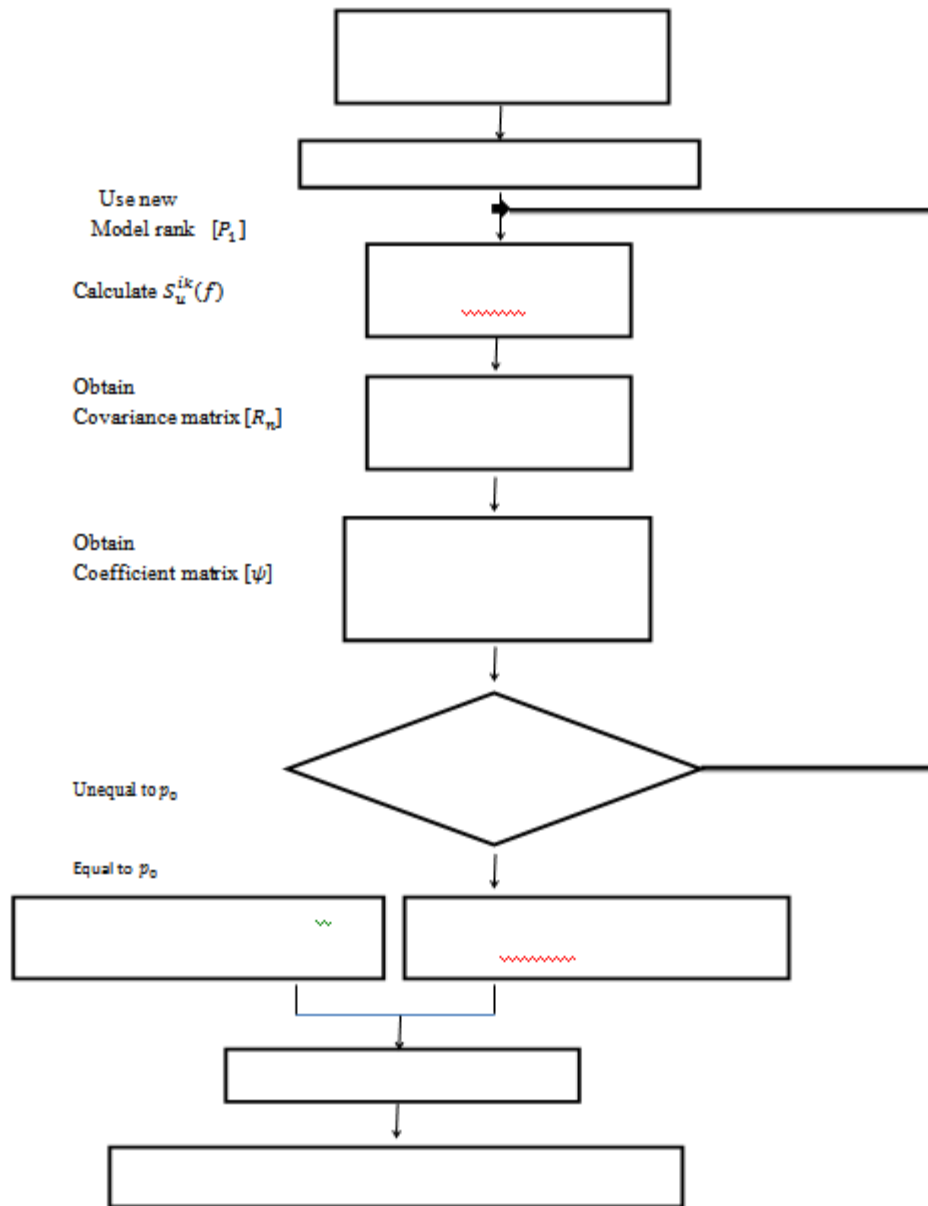
Figure 3.2: Flow chart of implementing wind velocity by AR model in Matlab

3.2.6.2 SOLVING THE NUMERICAL INTEGRAL EQUATION 3.7 WHICH CONTAINS OSCILLATING FUNCTION

The integral function of Eq. 3.7 contains the oscillating function $\cos(2\pi.f.j\Delta t)$. With the growth of the variable $2\pi.f.j\Delta t$, the integral function will have more points of zero value on x-axis coordinate. Then a general numerical interpolation can not meet the requirement of accuracy, and neither can the compound integral method. In this study, the Gauss-Lobatto formula improved from the Gauss formula is used to solve the integral of oscillation function. The formula can be expressed as [15]:

$$R_u = A_1 f(a) + A_n f(b) + \sum_{k=2}^{n-1} A_k f(x_k) + K_n f^{2n-2}(\xi) \quad ..... (3.17)$$

Where, a & *b* are the ends points of each range $A_1, ..., A_n$, K_n are $n + 1$ parmeters.

3.3 LEKKI CABLE BRIDGE WIND FIELD EVALUATIONS

Using those methods mentioned above, one can simulate the wind velocity at four-space points as shown in Fig 3.3. The parameters used in the simulation are: the roughness length, $z_o = 40m$, the standard mean component of the wind velocity, $\bar{v} = 28$ m/s^2, the discrete time $\Delta t = 0.1$ s. The results of the simulation are shown in Figs. 4.2.

C (0, 28, 10)

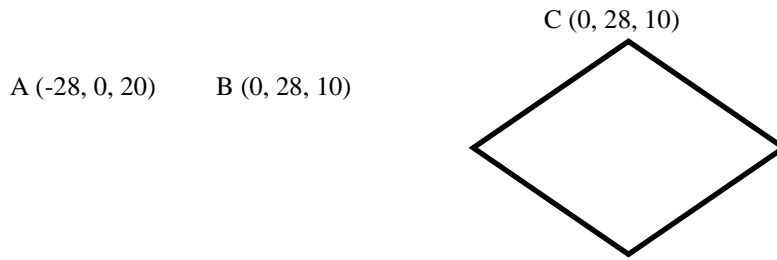A (-28, 0, 20)　　　B (0, 28, 10)

Figure 3.3: Four-space points (unit: m)

IV. RESULT
4.1 LEKKI CABLE BRIDGE WIND VELOCITY SIMULATION USING AR MODEL

The results below were based on typical average weather of Ikeja Lagos (bridge location), for the historical records from 2007 – 2012 where earlier records are either unavailable or unreliable. Ikeja has a tropical savannah climate and covered by forests (35%), oceans and seas (20%), marshes (18%), croplands (12%), and grassland (7%).
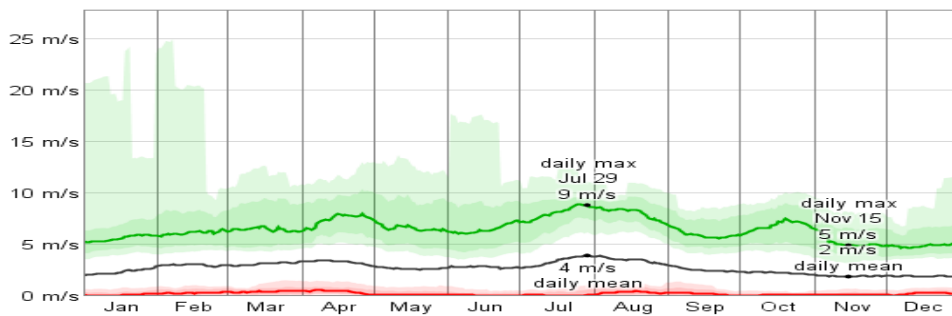
Figure 4.1: Ikeja average wind speed (Weatherspark.com)

Wind over the course of the year typical wind speeds vary from 0 m/s to 9 m/s (calm to fresh breeze), rarely exceeding 25 m/s (storm). The highest average wind speed of 4 m/s (gentle breeze) occurs around July, at which time the average daily maximum is 9 m/s (fresh breeze), and the lowest average wind speed of 2 m/s (light breeze) occurs around November, at which time the average daily maximum wind speed is 5 m/s (gentle breeze).
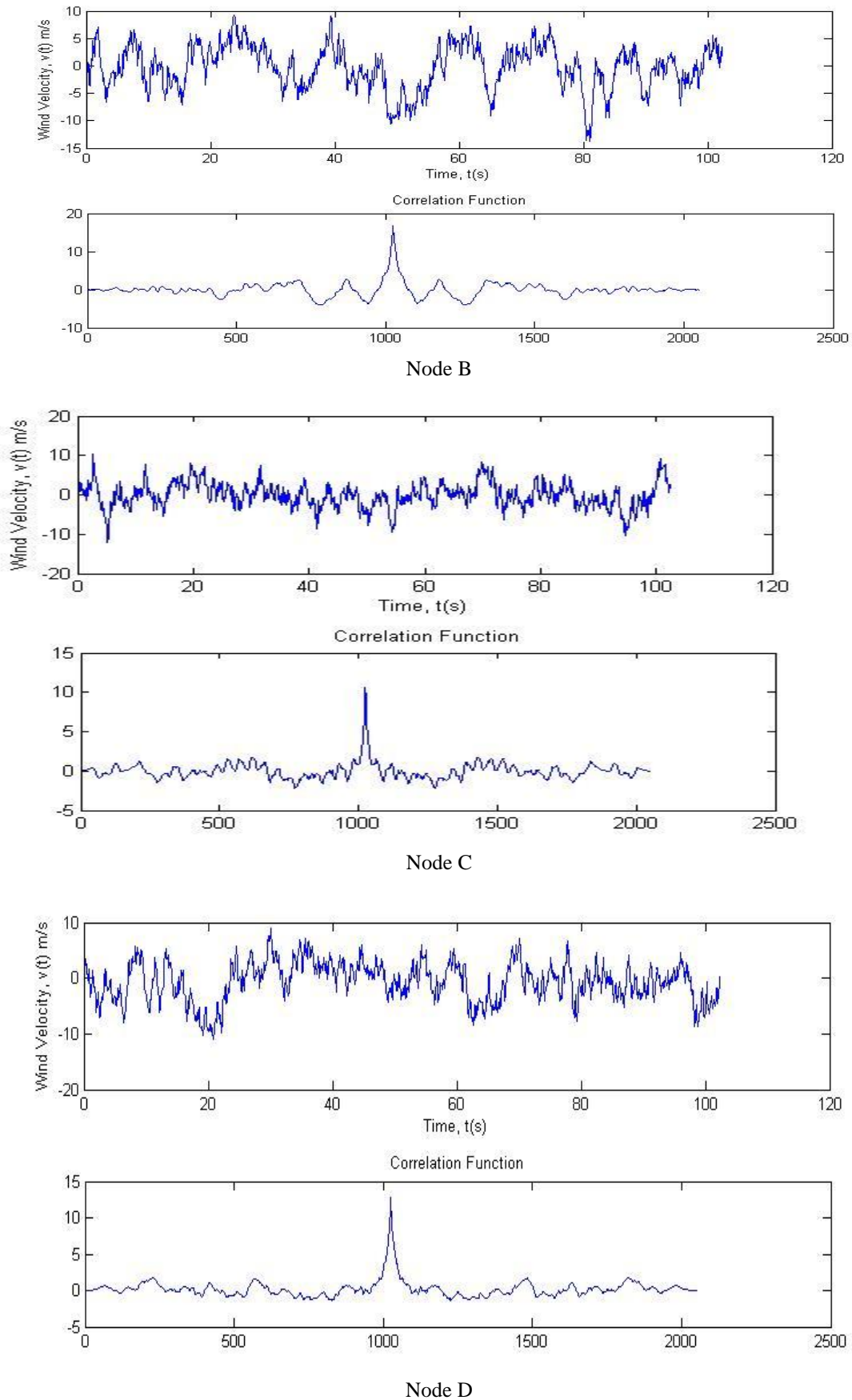
Node A

Node B

Node C

Node D
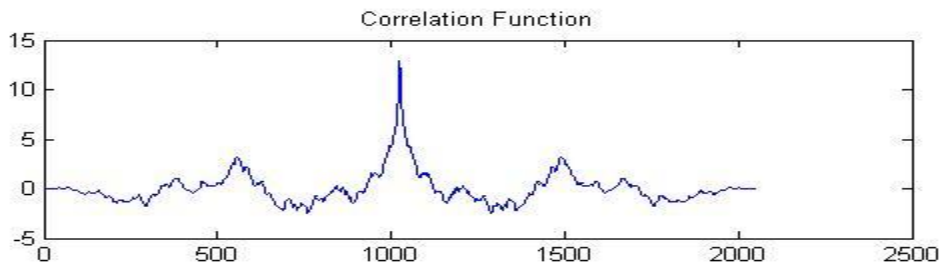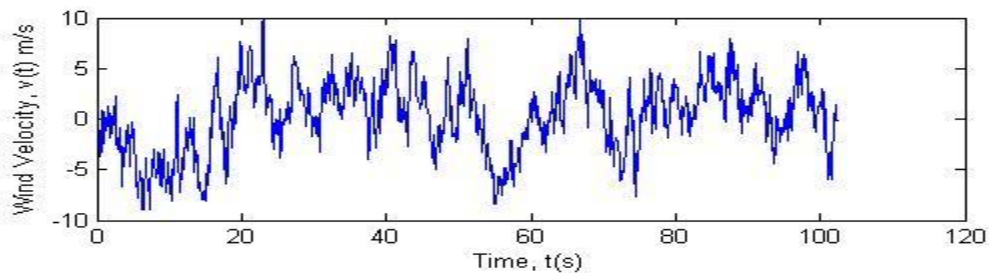
Figure 4.2: Wind velocity and correlation function simulated using AR Model.

4.2 DISCUSSION

Fig. 4.2 shows the fluctuating components of wind velocities at the four-space points, with the rank of the AR model P = 4. The wind velocity curves also illuminate that the wind velocity (10 to -15m/s^2) is a random process accompanying the varieties of time.

It further represents the type of random process; and describes certain time-varying processes in nature condition of the bridge.

V. CONCLUSION

From the results obtained in Fig. 4.2 above, the fluctuating components of the wind velocity which displays as (10 to -15m/s^2)by the fluctuant curve will result in the vibration of the structure, even strengthens the resonance effect of the structure. The autoregressive model specified that the output variable depends linearly on its own previous values and on a stochastic term.

VI. ACKNOWLEDNMENT

I would like to acknowledge Dr. Prashant Mukherjee, Dr. A. Mohammed, and Shashi Kant for their invaluable suggestions and inputs toward this research.

REFERENCES

[1]   Marco L., Vincenzo G., A Parametric multi body section model for model interactions of cable supported bridges, Journal of Sound and Vibration 333 (2014) 4579–4596.
[2]   A.M. Abdel-Ghaffar, M.A. Khalifa, Importance of cable vibration in dynamics of cable-stayed bridges, Journal of Engineering Mechanics 117 (11) (1991) 2571–2589.
[3]   P. Warnitchai, Y. Fujino, T. Susumpow, A non-linear dynamic model for cables and its application to a cable-structure system, Journal of Sound and Vibration 187 (4) (1995) 695–712.
[4]   S.H. Cheng, D.T. Lau, Modeling of cable vibration effects of cable-stayed bridges, Earthquake Engineering and Engineering Vibration 1 (1) (2002) 74–85.
[5]   R.H. Scanlan, The action of flexible bridges under wind, II: Buffeting theory, Journal of Sound and Vibration, Volume 60, Issue 2, 22 September 1978, Pages 201-211.
[6]   Iwatani, Y. 1982, Journal of Wind Engineering, 11, 5-14, Simulation of multidimensional wind fluctuations having any arbitrary power spectra and cross spectra.
[7]   Iannuzzi, A. and Spinelli, P. 1987, Journal of Structural Engineering, ASCE, 113(10), 2382-2398, Artificial wind generation and structural response.
[8]   Li, Y-Q and Dong, S-L. 2001, Spatial Structure, 7(3), 3-11, Random wind load simulation and computer program for large-span spatial structures (In Chinese).
[9]   Strube, H.W. 1985, Signal Process, 8(1), 53-74, A generalization of correlation functions and the Wiener-Khinchin theorem.
[10]   Schlindwein, F. S. and Evans, D. H. 1990, Ultrasound Med. Biol. 16(1), 81-91, selection of the order of autoregressive models for spectral analysis of Doppler Ultrasound signals.
[11]   Akaike, H. 1974, IEEE Trans. Automatic Control, 19, 716-723, A new look at the statistical model identification.
[12]   Pappas, S. S., Leros, A. K., and Katsikas S. K. 2006, Digital Signal Processing, 16, 782-795, Joint order and parameter estimation of multivariate autoregressive models using multi-model partitioning theory.
[13]   Martinsm M. M., Trigo, M. E., and Santos. M. M. 1996, Linear Algebra. Appl., 232, 131-147, an error bound for the SSOR and USSOR methods.
[14]   Gander, W. and Gautschi, W. 2000, Numerical Mathematics, 40, 84,101, Adaptive quadrature revisited.
[15]   Weicheng Gao and Yanlei Yu, Journal of Wind and Structure, vol. 11, No.3 (2008), pp. 241-256, Wind velocity simulation of spatial three-dimensional fields based on autoregressive model.

APPENDIX A
EXTERNAL FILE (COOR.TXT)

```
Coordinate data
Number of Coordinates N=3

x-data
-28 0 20

z-data
15 24 56
```

APPENDIX B
MATLAB SCRIPTS

```
clc
clear all
```

```
tic
P=4;
v10=36;
n=0.01:0.01:10;
xn=1200*n./v10;
k=0.00215;
ti=0.1;
s1=4*k*v10^2*xn.^2./n./(1+xn.^2).^(4/3);
syms plf;
fr = fopen('coor.txt', 'rt');
N = fscanf(fr, '%*s %*s\n%*s %*s %*s N=%d\n', 1);
fgetl(fr);
for i=1:N
    x(i)= fscanf(fr,'%f',[1,1]);
end
fgetl(fr);
fgetl(fr);
fgetl(fr);
for i=1:N
    z(i)=fscanf(fr,'%f',[1,1]);
    v(i)=(z(i)/10)^0.16*v10;
end

A=zeros(P*N);

for p=1:P

    R=zeros(N);
for i=1:N
for j=i:N


H=inline('(4*k*v10^2*(1200*f/v10).^2)./f./(1+(1200*f/v10).^2).^(4/3).*(exp(
-2*f*sqrt(8^2*dx.^2+10^2*dz.^2)/vt)).*cos(2*pi*f*(p-
1)*ti)','f','k','dx','dz','ti','v10','vt','p');
            vt=(v(i)+v(j));
            dx=x(i)-x(j);
            dz=z(i)-z(j);
            R(i,j)=quadl(H,0.01,10,0.001,0,k,dx,dz,ti,v10,vt,p);
            R(j,i)=R(i,j);
end
end

for l=1:P-p+1
        A(((l-1)*N+1):(l*N),((l+p-1-1)*N+1):((l+p-1)*N))=R;
end


end

for i=1:P*N
for j=1:i
        A(i,j)=A(j,i);
end
end
R=zeros(N);
for i=1:N
for j=i:N

H=inline('(4*k*v10^2*(1200*f/v10).^2)./f./(1+(1200*f/v10).^2).^(4/3).*(exp(
```

```
-
2*f*sqrt(8^2*dx.^2+10^2*dz.^2)/vt)).*cos(2*pi*f*P*ti)','f','k','dx','dz','t
i','v10','vt','P');
        vt=(v(i)+v(j));
        dx=x(i)-x(j);
        dz=z(i)-z(j);
        R(i,j)=quadl(H,0.01,10,0.001,0,k,dx,dz,ti,v10,vt,P);
        R(j,i)=R(i,j);
end
end
B=A(1:N,(N+1):(N*P));
B=[B,R];
B=B';
X=A\B;
R0=A(1:N,1:N);
RN=R0;
for i=1:P
    RN=RN-(X(((i-1)*N+1):(i*N),1:N))'*B(((i-1)*N+1):(i*N),1:N);
end
L=chol(RN);
L=L';
a=zeros(N,1024);
for i=1:N
    a(i,:)=normrnd(0,1,1,1024);
end

V(1:N,1)=L*a(:,1);
for i=2:p
    V(1:N,i)=L*a(:,i);
for j=1:i-1
        V(1:N,i)=(X(((j-1)*N+1):(j*N),:))'*V(1:N,(i-j))+V(1:N,i);
end
end

for i=(P+1):1024
    V(1:N,i)=L*a(:,i);
for j=1:P
        V(1:N,i)=(X(((j-1)*N+1):(j*N),:))'*V(1:N,(i-j))+V(1:N,i);
end
end
toc

V1=V(1,:);
t=(1:1024)*ti;
figure
subplot(2,1,1);
plot(t,V1,'b-');
xlabel('Time, t(s)');
ylabel('Wind Velocity, v(t) m/s');

[power,freq]=psd(V1,1024,10,boxcar(1024),0,'mean');
power=power*2/10;
subplot(2,1,2);
loglog(freq,power,'r-',n,s1,'g-');

maxlags=1024;
cx = xcorr(V1(1,:),V1(1,:),maxlags,'biased');
plot(cx)
fid=fopen('windv.dat','wt');
```

```
for i=1:1:1024
for j=1:1:N-1
      fprintf(fid,'%e \t',V(j,i));
end
    fprintf(fid,'%e \n',V(N,i));
end
fclose(fr);
fclose(fid);
```